

Engineering Notes

ENGINEERING NOTES are short manuscripts describing new developments or important results of a preliminary nature. These Notes cannot exceed 6 manuscript pages and 3 figures; a page of text may be substituted for a figure and vice versa. After informal review by the editors, they may be published within a few months of the date of receipt. Style requirements are the same as for regular contributions (see inside back cover).

Rain Simulation Studies for High-Intensity Acoustic Nose Cavities

R. M. Clayton,* Y. I. Cho,† P. Shakkottai,*
and L. H. Back‡
Jet Propulsion Laboratory
California Institute of Technology
Pasadena, California

Introduction

AXISYMMETRIC cavities of small sizes on the nose of unarmed plastic projectiles are considered attractive for the generation of intense tones for coding for a simulation of area weapons effects in training maneuvers.¹ Different whistles can represent different sizes of shells. The tones produced in flight are desired at velocities near the end of the trajectory at a low speed of about 65 m/s.

This Note is concerned with the simulation of rainfall in an airstream and the effect of rain droplet impingement on the nose of the projectiles, in particular, on any penetration or accumulation of water at the base of the cavity that might increase the fundamental cavity frequency and/or reduce the intensity of sound production during rain conditions. Tail-fin-stabilized and spin-stabilized projectiles are of interest.

Strobe silhouette photographs and pictures taken with front lighting are included to acquire visual information on the spatial distribution of the drops in the airstream, drop impingement bead/sheet characteristics on the nose of the projectiles, and water droplet characteristics at the mouth of the cavity—which is not well understood, especially with periodic eddy shedding from the resonant cavity.

System Rationale

Simulation of rainfall in a moving airstream is difficult since it is necessary to provide simultaneously a given monodisperse droplet size and a given droplet spacing to simulate a particular precipitation intensity. It is inherent with conventional pressure atomizing spray nozzles that: 1) monodisperse droplet sizes are not produced and 2) droplet spacing is much too small.

Typical water dispersion schemes for rain simulation in wind tunnels utilize high-pressure feed systems in order to inject water through tubular nozzles coaxially with the airstream at nearly the prevailing air velocity and thus reduce the effect of slip velocity on droplet breakup. Provisions for specific droplet size and droplet spacing are then typically controlled by the size of the tubular nozzles and their spatial position in the cross section of the airstream. Such a system is described in Ref. 2.

For the experimental program of interest here, a simple, less expensive means was desired to simulate precipitation in the range of drizzle to heavy rain in an airstream. The blower/nozzle geometry for the acoustic nose cavity experiments together with some pertinent airflow parameters are shown in Fig. 1. The air velocity was 213 ft/s (65 m/s).

As is seen from Fig. 1, the volumetric airflow at the desired experimental condition is 29 ft³/s (0.82 m³/s). Pertinent rain intensity definitions from Ref. 2 when applied to the stated airflow give required droplet sizes of 200–1500 μ m and droplet spacing of 1.75–6.28 in. (44.5–159.5 mm) for drizzle to heavy-rain conditions, respectively. These conditions also correspond to a water mass flow rate of 0.59–5.44 lbm/h (4.49–41.1 cm³/min) and a droplet number density of 615–13 drops/ft³ (21,700–459 drops/m³), respectively. For a given rain intensity, the requirements for water flow rate, droplet size, and droplet spacing should be approximated simultaneously.

Rains above the intensity of a drizzle are more difficult to simulate because high air velocity tends to shatter droplets to sizes down into the range of fogs, mists, and drizzles unless the larger droplets are initially formed at liquid velocities near the test condition airspeed so that they are exposed to low slip velocities. This requires an expensive high injection pressure or an alternate injection/atomization approach.

An alternate approach is suggested by the work reported in Ref. 3. Experimental results from Ref. 3 under conditions similar to the present test setup show that the accelerating flow between the honeycomb and the outlet cone should reduce the mass median droplet size from an initial size of 400–600 μ m to about 150 μ m at the outlet. This 150 μ m size approximates the drizzle intensity; thus, it was decided to use this condition as a baseline design condition for the rain simulation system.

The resulting apparatus comprised a small positive-displacement pump and a water injection array located in the low airspeed region downstream of the honeycomb (Fig. 1) to distribute the water flow as evenly as practical across the 5 in. (12.7 cm) diameter of the outlet air jet. Nine individual injection tubes were fed by a common circular manifold (Fig. 1). The tubes were fabricated of 0.009 in. (0.23 mm) diameter hypodermic needles.

The configuration described above introduces water at the drizzle condition with negligible velocity into a coflowing airstream with a velocity of 27 ft/s (8.2 m/s). The Nukiyama-Tanasawa correlation⁴ can be used to estimate mean droplet size for this flow configuration,

$$d_{32} = \frac{585}{V_R} \left(\frac{\sigma_t}{\rho_t} \right)^{0.5} + 597 \left(\frac{\mu_t}{\sigma_t \rho_t} \right)^{0.225} \left(\frac{Q_t \times 10^3}{Q_a} \right)^{1.5} \quad (1)$$

where σ_t is the water surface tension in dynes/cm, ρ_t the water density in g/cm³, μ_t the water viscosity in poise, Q_a the air volume flow rate, Q_t the water volume flow rate, V_R the relative slip velocity in m/s, and d_{32} the Sauter mean diameter in μ m.

Equation (1) predicts a mean droplet size of 630 μ m at the water injection station on the downstream side of the honeycomb section. Thus, a droplet size of about 150 μ m might be expected at the outlet cone after further breakup due to the accelerating flow.

Received April 20, 1987; revision received June 8, 1987. Copyright © American Institute of Aeronautics and Astronautics, Inc., 1987. All rights reserved.

*Member of Technical Staff. Member AIAA.

†Member of Technical Staff; currently with Drexel University, Philadelphia. Member AIAA.

‡Technical Group Supervisor. Associate Fellow AIAA.

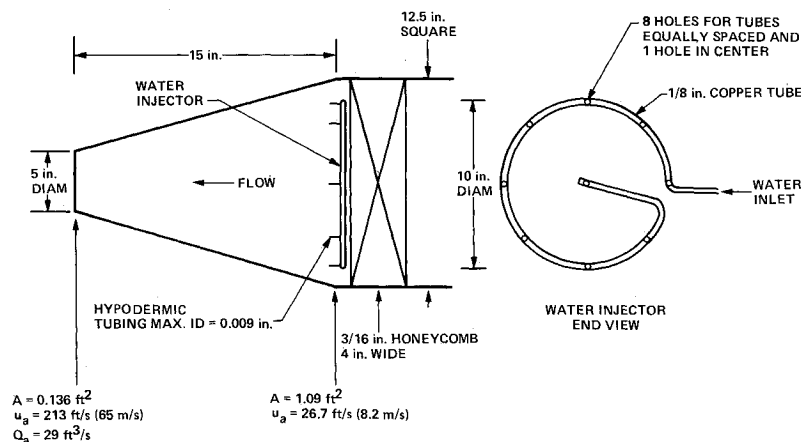


Fig. 1 Blower nozzle geometry and water injector.

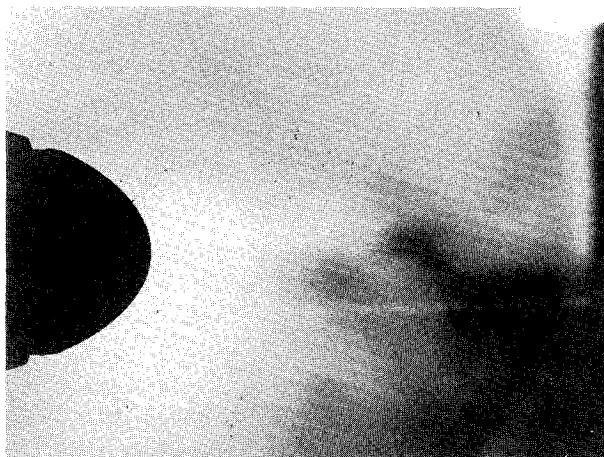


Fig. 2 Silhouette photograph for test 41 at a rain simulation water flow rate of $77 \text{ cm}^3/\text{min}$ (liquid water content $m_w/V_a = 1.55 \times 10^{-6} \text{ g/cm}^3$).

Experiments

The drops were photographed in silhouette. A point stroboscopic light source illuminated a Fresnel lens that gathered the light and directed it into a camera lens. The jet flow and droplets were present in the converging cone of light. The camera focused on the backlit drops. At a typical f number equal to 22, the depth of field was approximately 0.5 in. (1.3 cm). During the experiment, the strobe lamp was flashed once as the camera shutter was opened. The camera exposure was much larger than the duration of the flash of light which was $1 \mu\text{s}$ at 0.1 J flash intensity. This short-duration light flash freezes the motion of droplets and thus provides data on the instantaneous spatial location and size of the droplets. Pictures were also taken with steady front lighting using a shutter speed of $1/500 \text{ s}$. At this speed, the motion of drops is not frozen and streak pictures are produced.

Analysis of the silhouette negatives was carried out using a De-Anza ID-5400 image processing system. The negative was placed on a light table in view of a video camera. The analog signal from the video camera was digitized and fed directly to an array processor that controlled the data flow and wrote the data into memory at a rate of 30 frames/s in a 512×512 pixel matrix. Images were stored on a mass storage device for processing using a PDP 11/34 minicomputer. Available software operations included image enhancement, filtering, drop contour detection and shape analysis, and drop size determination. The system had previously been applied to the analysis of fuel sprays.⁵

All the experiments were conducted at the 213 ft/s (65 m/s) airspeed and with the projectile (RB-20-0) aligned coax-

ially with the airstream. Water flow rates of 0.40, 4.0, and 10.2 lbm/h (3, 30, and $77 \text{ cm}^3/\text{min}$) were used to span the range from light to heavy precipitation. Photographic results and the computerized analysis of the results will be discussed.

Results

Figure 2 is a silhouette photograph at the higher rain simulation water flow rate of $77 \text{ cm}^3/\text{min}$ (test 41). The flow is from right to left. The projectile nose silhouette delineates the mouth of the axisymmetric ring cavity located at a radius of 1.88 cm (length scale for the picture) where the ratio of local freestream velocity to jet velocity is 1.16. The cavity depth is 1.93 cm. The nose shape is an ellipse with ratio of major-to-minor axes of two. Water droplet silhouettes for the instant of time photographed indicate a number of interesting features. The droplets are of variable size, presumably due to the breakup of larger drops in the flow acceleration section upstream and in the jet. Table 1 gives values of the arithmetic mean droplet diameter d_{10} and the volume-surface mean diameter d_{32} for those drops processed for this test, the values being about 280 and $380 \mu\text{m}$, respectively. Many more droplets out of focus appear smaller and fuzzy and were not processed. In comparison to fuel sprays in combustors, the water droplet spacing associated with rain simulation is relatively large, so that image processing of instantaneous droplet silhouettes such as obtained herein for the field of view and droplets in sharp focus involved relatively few drops, as indicated in Table 1. Correspondingly, the average liquid water content m_w/V_a (in gm/cm^3) obtained by dividing the water mass flow rate by the air volume flow rate is extremely small, being about 10^{-6} the density of water as noted in Table 1, which is typical of rain. The droplets were instantaneously nonuniform across the flow. This is indicative of the relatively few droplets in the flow, but is also probably associated with some clustering of sibling drops produced in the larger-drop breakup process.

Information on other tests that were image processed is given in Table 1, there being three other tests at the same liquid water content as for test 41 and two tests at a lower water flow rate $30 \text{ cm}^3/\text{min}$ with a corresponding lower liquid water content, as noted. The column $\mu\text{m}/\text{pixel}$ relates to the particular pixel matrix calibration with actual size. Mean droplet diameters d_{10} and d_{32} are seen to be variable for photographic silhouettes at the same water flow rate and at the lower water flow rate. In particular, the average value of d_{10} for the number of drops processed for the tests at a water flow rate of $77 \text{ cm}^3/\text{min}$ was about $320 \mu\text{m}$. For the drizzle condition $\dot{Q}_w = 3 \text{ cm}^3/\text{min}$ and $m_w/V_a = 0.06 \times 10^{-6} \text{ g/cm}^3$, there were only a couple of drops in the silhouette photograph.

Figure 3 is a picture with front lighting at the higher rain simulation flow rate of $77 \text{ cm}^3/\text{min}$ (test 46). In this case,

Table 1 Summary of rain simulation image processing

Test	\dot{Q}_w , cm ³ /min	Liquid water contents m_w/V_g , g/cm ³	Projectile, rpm	$\frac{\mu\text{m}}{\text{pixel}}$	No. of drops		
					processed	d_{10} , μm	d_{32} , μm
30C	30	0.60×10^{-6}	0	23	8	367	420
31A	30	0.60×10^{-6}	0	23	15	227	312
33A	77	1.55×10^{-6}	0	23	9	368	416
33D	77	1.55×10^{-6}	0	23	16	390	671
40	77	1.55×10^{-6}	8000	21	9	265	332
41	77	1.55×10^{-6}	0	21	26	278	378

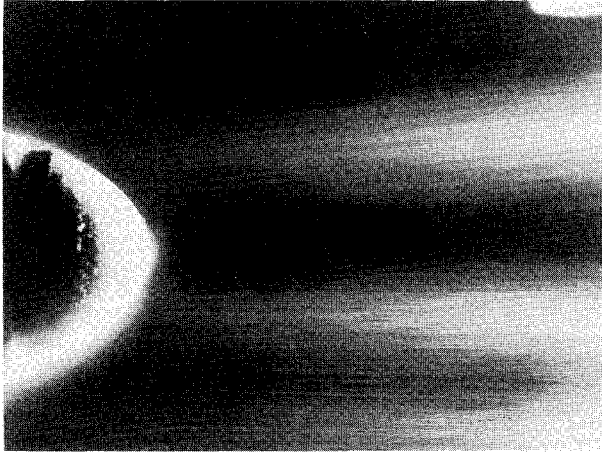


Fig. 3 Photograph with front lighting for test 46 at a rain simulation water flow rate of 77 cm³/min (liquid water content $m_w/V_a = 1.55 \times 10^{-6}$ g/cm³).

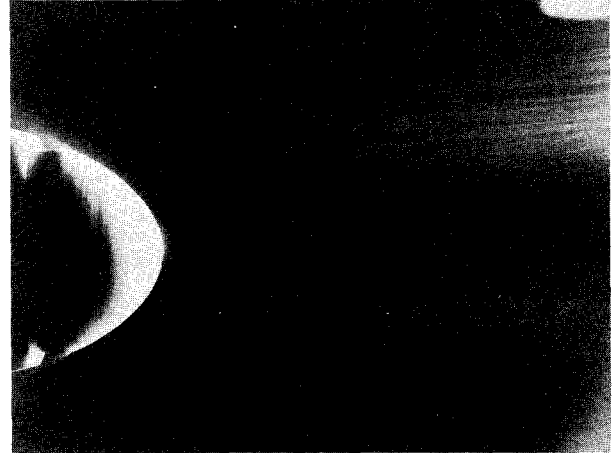


Fig. 4 Photograph with front lighting for test 42 at a rain simulation water flow rate of 30 cm³/min (liquid water content $m_w/V_a = 0.60 \times 10^{-6}$ g/cm³, spinning projectile at 8000 rpm).

the droplet trajectories appear as streaks. Droplets impinging on the projectile upstream of the cavity appear as beads of water on the nose surface and are nearly round and uniform in size, being about 400 μm . Streaks appear at the cavity mouth associated with a fine water spray from the upstream nose, which was better seen in other silhouette pictures. Visual observation during the test indicated some accumulation of clumps of water at the mouth of the cavity that would oscillate, but not penetrate into the cavity.

Figure 4 is a picture with front lighting at the intermediate rain simulation flow rate of 30 cm³/min for the case of a spinning projectile at 8000 rpm. In this case, the streaks are fewer because of the lower liquid water content and thus fewer drops. With spin, a liquid water sheet formed on the nose of the projectile and surface waves were also evident. At the cavity mouth, there occurred a fine water spray similar to the nonspinning case (Fig. 3), but it was less dense because of the lower liquid water content.

For all of the rain simulation tests, there was no change in the high-intensity tone generation emanating from the mouth of the cavity compared to tests with no rain. The acoustic resonance frequency of 4.6 kHz for this particular cavity configuration (RB-20-0)¹ remained the same with rain simulation. During each cycle of resonant motion, the eddy leaving the cavity (see Ref. 1, Fig. 17) was apparently strong enough to prevent penetration and accumulation of water at the base of the cavity that might increase the fundamental cavity frequency and/or change the intensity of sound production.

In conclusion, the rain simulation study using hypodermic needles revealed smaller drops on the order of 300 μm compared to millimeter size drops in moderate-to-heavy precipitation for the same liquid water content, but the observed droplet size was more than twice as large as that

estimated from prior experimental results and correlations. The high-intensity tone generation produced at the mouth of the ring cavity on the nose of the projectile was unaffected by the rain simulation. These results apply to simulation of light precipitation in terms of mean drop size, although the liquid water content extended to that for heavy precipitation, so that there were many more drops but they were smaller in size compared to natural heavy rain.

Acknowledgment

The work described in this Note was carried out by the Jet Propulsion Laboratory, California Institute of Technology, and was sponsored by the U.S. Army through an agreement with NASA.

References

- Shakkottai, P., Kwack, E.Y., Cho, Y.I., and Back, L.H., "High Intensity Tone Generation by Aeroacoustic Sources," *Journal of the Acoustical Society of America*, Vol. 82, 1987, pp. 2075-2085.
- Melene, H.R., "Rain Simulation in Wind Tunnels," Gull Engineering, Inc. Report, Oct. 1967.
- Zajac, L.J., "Droplet Breakup in Accelerating Gas Flows, Part II: Secondary Atomization," NASA CR-124479, Oct. 1973.
- Nukiyama, S. and Tanasawa, Y., "Experiments of the Atomization of Liquids in an Air Stream," Defense Research Board, Dept. of National Defense, Ottawa, Canada, March 19, 1950 [translated from *Transactions of the Society of Mechanical Engineers (Japan)*, Vols. 4-6, 1938-1940, by E. Hope].
- Fleeter, R., Toaz, R., and Sarohia, V., "Application of Digital Image Analysis Techniques to Antimisting Fuel Spray Characterization," ASME Paper 82-WA/HT-23, Nov. 1982.